Design and development of a mixed alcoholic beverage kinetics using asaí (*Euterpe precatoria*) and copoazú (*Theobroma grandiflorum*)

Diseño y desarrollo de una cinética de bebida alcohólica mixta de asaí (*Euterpe precatoria*) y copoazú (*Theobroma grandiflorum*)

Willian Quintero Mendoza[1], Raquel Oriana Díaz-Salcedo[2*], and María Soledad Hernández-Gómez[1, 2]

ABSTRACT

Copoazú (*Theobroma grandiflorum*), a fruit from the same genus as cacao, and asaí (*Euterpe precatoria*) a palm fruit, both of Amazonian origin, could promote local economic growth through fruit processing to increase the added value. This study aimed to identify the kinetics of alcoholic fruit beverages made from copoazú and asaí pulp or seeds, *i.e.*, the fermentation kinetics in the case of copoazú drinks and the diffusion kinetics in the case of asaí drinks. Additionally, the feasibility of generating a milky mixture with the liquor obtained from the copoazú fruit processing was evaluated. Statistical analysis was performed by ANOVA tests and modeling of kinetics parameters with an evolutionary algorithm and optimization. Copoazú pulp was fermented with 15% Prestige Turbo Yeast®. Fermentation was separated into two stages: controlled fermentation during the first 5 d and a maturation process in the following 25 d. According to the modeling, the greatest efficiency was observed with 600 g L^{-1} pulp concentration and soluble solids adjusted at 35°Brix, with alcohol contents of up to 20% (w/v) after 30 d of processing and evidence that there may be inhibition of fermentation due to glycerol. The whole fruit and pulp of asaí were extracted with ethanol to obtain a liquor with the micronutrients and flavors of the fruit, and the anthocyanin content was used as a degradation process marker. Modelling showed that the optimum point that yielded maximum anthocyanin concentration was achieved at 60 d of maturation by extracting pulp in a 45% (w/v) ethanol solution resulting in a maximum anthocyanin content of 94.2 ± 15.3 mg of cyanidin-3-glucoside kg^{-1} of liquor. After that, a degradation process was observed as anthocyanin content diminished.

Key words: Amazonian fruits, modelling, fermentation, diffusion.

RESUMEN

El copoazú (*Theobroma grandiflorum*), una fruta del mismo género que el cacao, y el asaí (*Euterpe precatoria*) una fruta de palma, ambas de origen amazónico, podrían promover el crecimiento económico local a través de su procesamiento para aumentar el valor agregado. El objetivo de este estudio fue identificar la cinética de las bebidas alcohólicas elaboradas con pulpa o semillas de copoazú y asaí, es decir, la cinética de fermentación en el caso de las bebidas de copoazú y la cinética de difusión en el caso de las bebidas de asaí. Además, se evaluó la viabilidad de generar una mezcla láctea con el licor obtenido del procesamiento del fruto del copoazú. El análisis estadístico se realizó con pruebas ANOVA y el modelamiento de los parámetros de las cinéticas con un algoritmo evolutivo y optimización. La pulpa de copoazú se fermentó con levadura Prestige Turbo® al 15%. La fermentación se separó en dos etapas: fermentación controlada en los primeros 5 d y un proceso de maduración en los siguientes 25 d. De acuerdo con el modelamiento, la mayor eficiencia se obtuvo con una concentración de 600 g L^{-1} y sólidos solubles ajustados a 35°Brix, con contenidos de alcohol de hasta 20% (p/v) después de 30 d de procesamiento y evidencia de la inhibición de la fermentación debida al glicerol. Un proceso de extracción etanólica de los frutos completos y pulpa de asaí se utilizó para obtener un licor con los micronutrientes y sabores de la fruta, y se usó el contenido de antocianinas como marcador del proceso de degradación. El modelamiento mostró que el punto óptimo se alcanzó tras 60 d de maduración al extraer la pulpa en una solución de etanol al 45% (p/v), alcanzando una concentración máxima de antocianinas de 94.2 ± 15.3 mg de cianidina-3-glucósido kg^{-1} de licor. Luego de esto, se observó un proceso de degradación al disminuir el contenido de antocianinas.

Palabras clave: frutos amazónicos, modelamiento, fermentación, difusión.

[1] Instituto de Ciencia y Tecnología de Alimentos - ICTA, Facultad de Ciencias Agrarias, Universidad Nacional de Colombia, Bogotá (Colombia).
[2] Instituto Amazónico de Investigaciones Científicas SINCHI, Leticia, Amazonas (Colombia).
* Corresponding author: rdiaz@sinchi.org.co

Introduction

A mixed alcoholic drink or cocktail is obtained by mixing one or more alcoholic liquids or food-grade ethyl alcohol, either with an agricultural origin of simple alcoholic distillates or with other beverages, such as fruit juice, macerated fruits, syrups, milk, eggs, or other animal or plant-based substances. The alcohol level in these drinks can range between 0.4 and 40 alcoholic degrees (Wardencki, 2019). In general, skills, supplies, and knowledge of food technology and other disciplines are needed to prepare these drinks and achieve a suitable mixture with pleasant sensory properties. Alternatively, an alcoholic drink could be mixed in a bottle dispenser, possibly with two different alcoholic beverages designed for subsequent mixing. In this study, the first drink was made with asaí, a neotropical palm fruit of Amazon origin with grape-shaped berries and a dry and oleaginous pulp that has a high content of antioxidants, such as anthocyanins, and a low amount of carbohydrates (Castillo *et al.*, 2012). This means that alcoholic fermentation cannot be carried out without adding sugars; therefore, this fruit was used to make an infused liquor. On the other hand, copoazú, a fruit from the *Theobroma* genus, like cacao and also of Amazon origin, has a higher content of carbohydrates in its pulp than fruits in the same class, which allows alcoholic fermentation (Duarte *et al.*, 2010). Its profile of acids and sugar contents allows for mixing milk with the resulting liquor according to the bromatological composition (Tab. 1). The asaí and copoazú liquor extracts can be mixed in a cocktail.

This study aimed to identify the kinetics of alcoholic fruit beverages made from copoazú and asaí pulp, *i.e.*, the fermentation kinetics in the case of copoazú drinks and the diffusion kinetics in the case of asaí drinks. Predicting the behavior of these drinks during preparation would facilitate correct decision-making for production conditions and provide the best quality product for subsequent cocktail preparation, thus avoiding an excessive number of trials and wasting raw materials (Wardencki, 2019).

A fermentation kinetic model was developed from the Monod model for copoazú alcoholic beverages because of its ability to represent microbial behavior, providing modifications for particular processing conditions (Gao *et al.*, 2018; Miller & Block, 2020). On the other hand, a diffusive process was used for the asaí alcoholic beverages, which is the most appropriate for modeling with Fick's law, using the continuity equation and considering degradation factors, interactions, and diffusion of the main component as a follow-up to the variable anthocyanin content (Chung *et al.*, 2016; 2017; Miller & Block, 2020).

Materials and methods

Fruits

Asaí and copoazú fruits were purchased from local producers in the Department of Amazonas. Ripe, washed, packed whole, or pulped fruits were selected at the agroindustry pilot plant of the SINCHI Institute in the city of Leticia, and sent to Bogotá properly refrigerated to perform the experiments.

Copoazú must preparation

Copoazú fruit pulp was diluted with water at varying concentrations between 400 and 600 g L^{-1} and adjusted with a

TABLE 1. Nutritional content of asaí and copoazú (modified from Cuellar Álvarez *et al*. (2017), Carrillo Bautista *et al*. (2016); Carrillo Bautista *et al*. (2017), Castillo *et al*. (2012) and Castillo Quiroga *et al*. (2017)).

Nutrient	Unit	Asaí		Copoazú	
		Pulp	Seed	Pulp	Seed
Fat	g/100 g	36.96	15.04	3.60	32.80
Fiber	g/100 g	42.43	36.29	16.00	22.00
Carbohydrates	g/100 g	18.28	NS	52.30	30.90
Protein	g/100 g	0.03	0.06	10.90	11.50
Calories	kcal	284.90	464.50	284.90	464.50
Ash	mg/100 g	2290	2600	232.10	689.90
Anthocyanins (Cyanidin 3-glucoside)	mg kg^{-1}	1136.31 $\pm$ 204		12.84 $\pm$ 0.39	
β-Carotene	mg/100 g	7.45		2.44 $\pm$ 0.47	
Citric acid	mg/100 g	NS		2186.90 $\pm$ 198.70	
Malic acid	mg/100 g	NS		49.20 $\pm$ 43.20	

NS - Not specified.

sucrose solution to 15, 25, or 35°Brix (Duarte *et al.*, 2010; Dias *et al.*, 2017; Wardencki, 2019) as shown in Table 2. These tests were performed in triplicate.

TABLE 2. Design of the copoazú alcoholic beverage fermentation experiment.

Trial	Substrate concentration (g L^{-1})	Soluble solids (°Brix)
A	400	15
B	400	25
C	400	35
D	600	15
E	600	25
F	600	35

Fermentation trials

Each must was fermented in 3 L batches for 5 d using 15% Prestige Turbo Yeast, *Saccharomyces cerevisiae*, controlling the temperature at 22°C. The pH was adjusted to 4.5 by adding calcium carbonate, and potassium metabisulfite to inhibit bacterial growth at a concentration of 100 g L^{-1} of free sulfur dioxide (SO_2) (Duarte *et al.*, 2010; Dias *et al.*, 2017). The fermented must was then matured for 25 d and the slurry was removed every 5 d, adding fresh water to replace the retired volume, and keeping the batch always at 3 L volume.

Infusion trials

Asaí fruit or pulp was mixed with extra neutral alcohol at a concentration of 15% (w/v), varying the concentration: 15, 30, or 45% (w/v) for the diffusion process as seen in Table 3. The infusion was kept in a maturation process for 90 d, and samples were collected on days 1, 2, 4, 8, 15, 30, 60, and 90 since the phenomenon of diffusion lessens over time, meaning that more time is needed between measurements to observe changes in the concentration of the analytes of interest in the beverage.

TABLE 3. Experiment design for the asaí alcoholic beverage formulation.

Formula	Asaí pulp (%)	Asaí fruit (%)	Water (%)
A	15	0	75
B	30	0	60
C	45	0	45
D	0	15	75
E	0	30	60
F	0	45	45

Analytical methods

Fermentation kinetics

The Monod model was used to model the behavior of the sugar contents, biomass, and ethanol concentration, with some variations to inhibit microorganisms with ethanol and glycerol. The following differential equations were used to observe variations in the three factors in fermentation and an equation for inhibition of the specific growth rate (Kumar *et al.*, 2013; Comelli *et al.*, 2016; Miranda Castilleja *et al.*, 2017):

Biomass:
$$\frac{dx}{dt} = x\mu e^{-\frac{K_L S_a}{t}} \tag{1}$$

Substrate:
$$\frac{dS}{dt} = -\frac{\mu}{Y_{\frac{x}{S}}} x e^{-\frac{K_L S_a}{t}} \tag{2}$$

Ethanol:
$$\frac{de}{dt} = \left(Y_{\frac{e}{x}}\mu x + \gamma x\right) e^{-\frac{K_L S_a}{t}} \tag{3}$$

Specific growth rate:
$$\mu = \frac{\mu_{max} S}{S + K_S + K_i S^2} \tag{4}$$

Where K_i is the inhibition constant expressed in L g^{-1}, K_s is the saturation constant expressed in g L^{-1}, K_L is the lag constant expressed in L h g^{-1}, μ is the specific growth rate expressed in h^{-1}, μmax is the maximum specific growth rate expressed in h^{-1}, $Y_{x/S}$ is the interaction between the biomass and substrate (adimensional), $Y_{e/x}$ is the interaction between the ethanol and substrate (adimensional), S is the substrate content expressed in g L^{-1}, x is the biomass content expressed in g L^{-1}, is the ethanol content expressed in g L^{-1}, γ is the ethanol production kinetic constant expressed in h^{-1}, S_a is the amount of sugar added expressed in g L^{-1}, and t is the time expressed in h.

Regression was used on the experimental data, finding the inhibition constant, the saturation constant, the lag constant, and the maximum specific growth rate with an evolutionary model that minimized the differences between theoretical and experiment data (Kumar *et al.*, 2013; Comelli *et al.*, 2016; Miranda Castilleja *et al.*, 2017). Subsequently, linear regression was used to calculate the interaction between the biomass and substrate and the interaction between the ethanol and substrate with the graphical representation x_i-x_0 vs. S_i-S_0, where the slope of the line was $Y_{x/S}$ and graphing e_i-e_0 vs. x_i-x_0 showed $Y_{e/x}$; these graphs resulted in several lines, each corresponding to a processing condition, which was proportional to the amount of added sugar (Comelli *et al.*, 2016).

Total soluble solids and biomass content

The fermentation kinetics were observed by measuring the total soluble solids (°Brix) every 30 min with an Atago PAL-1 pocket refractometer (Atago, Japan). For the biomass, the optical density of the must was measured every 30 min by taking 1 ml of sample and placing it in a quartz cell, with the measurement taken at a wavelength of 600 nm in a Thermo Scientific Evolution 60S UV-Visible spectrophotometer (Thermo Fisher Scientific, USA), following the adjusted methodologies of Bermejo et al. (2011).

Alcohol content

A sample of the liquid phase was taken from the fermenter and placed in a cylinder, covering the alcoholometer (ECO, Spain) but allowing the contents to move around freely. The alcoholometer was immersed, gently rotated, and left to stabilize. The corresponding reading was taken in the lower meniscus, according to Miller (2019), as adapted for fruit wines.

Infusion kinetics

Anthocyanin content

The infusion kinetics were observed by measuring the anthocyanin content of the asaí infusion, following the methodology of Li et al. (2017), modified for the measurement of infusion liquors. One hundred mg of the sample was weighed in triplicate and 5 ml of analytic grade methanol, acidified with 5% formic acid, was added. Each mixture was vortexed for 10 min and centrifuged for 45 min at 15,000 rpm. Two hundred µl of supernatant was taken and the pH was adjusted to 1.0 (0.025 M KCl buffer) and 4.5 (0.4 M Sodium acetate buffer), adding 2 ml of the buffer in each case. This measurement was obtained in triplicate using a Thermo Scientific Evolution 60S UV-Visible spectrophotometer (Thermo Fisher Scientific, USA) at the wavelengths 520 nm and 700 nm. Finally, the anthocyanin content was calculated using the following equation:

$$C = \frac{PM \times V \times (A_{520nm} - A_{700nm})_{pH = 1.0} - (A_{520nm} - A_{700nm})_{pH = 4.5}}{P \times \varepsilon}$$

(5)

where PM is the molar weight of cyanidin-3-glucoside (449.2 g /mol), ε is the molar extinction coefficient (25.964 /mol cm^{-1}), P is the sample's fresh weight, V is the volume of added methanol, A is the absorbance at each pH and wavelength, and C is the anthocyanin content [mg of cyanidin-3-glucoside kg^{-1}] (Salaha et al., 2008; Li et al., 2017; Li et al., 2018).

Oxidative rancidity (Fat acidity index)

The methodology described by the United States Pharmacopeial Convention (2013) was followed to determine this index, in which 2.5 g of the fresh sample was weighed in an Erlenmeyer flask, to which 50 ml of a mixture of alcohol and ether was added at a 1:1 w/w ratio (this mixture was neutralized with 0.1 N potassium hydroxide, observing the turning point with phenolphthalein). The homogeneous mixture was titrated with 0.1 N potassium hydroxide until the solution was slightly pink for 30 sec. The acid number was the number of hydroxide ions necessary to neutralize 10 g of sample, calculated as follows:

$$Oleic\ Acid\ \% = \frac{282.4 \times V \times N}{W} \times 100$$

(6)

where 282.4 is the molecular weight of oleic acid, V is the volume in ml, N is the normality of the potassium hydroxide solution, and W is the fresh weight of the sample (United States Pharmacopeial Convention, 2013).

Profile of sugar and organic acids

High-Performance Liquid Chromatography (HPLC) was used to measure the organic acids. First, 100 mg of sample was weighed and extracted with 3 ml of 5 mM sulfuric acid for 10 min in a Vortex. Then, the solution was centrifuged at 10,000 rpm for 45 min. Finally, the remaining liquid was removed, which was filtered with 0.45 µm PTFE membranes before injection in an Aligent 1200 Series HPLC (Aligent, USA). A 300 mm x 7.8 mm HPX-87H column was used, with a refractive index detector (RID) and diode array detector (DAD), 5 mM sulfuric acid as the mobile phase, and a flow of 0.5 ml/min. The peaks were detectable at 243 nm (Topalovic & Mikulic-Petkovsek, 2010).

Statistical data analysis

For the analysis of variance, the data obtained in triplicate in each variable were processed in IBM SPSS Statistics 25 with an ANOVA test finding significant differences between the treatments with a probability of 95%. Matlab 2019b was used for the parameters of the kinetic equations, optimizing the parameters with an evolutionary algorithm and the optimization toolbox sandbox, which progressively minimized the differences between the theoretical and experimental data.

The data were analyzed to determine the parameters of each kinetic, fermentation kinetics for the copoazú, and diffusion kinetics for the asaí. The kinetics were determined for

the most appropriate process parameters in each case to subsequently mix both liquors.

Results and discussion

Fermentation kinetics

Sugar and organic acid profile

The liquors had a relatively high content of citric acid (Tab. 4), which was consistent with these fruits, while the content of other acids was due to the acid transformation in the reactions of the citric acid cycle activated in the reoxidation of NADH to NAD^+. This is also because the glycolysis reactions were maintained since, under anaerobic conditions, NAD^+ is regenerated through the conversion of pyruvate to lactate by lactate dehydrogenase. This conversion was probably the result of lactic acid bacteria present in most naturally. This production can significantly increase the acidity of a wine as well as result in soft aromas and a sweet flavor, improving the sensory profile for subsequent mixing with milk for cream liqueurs (Vasantha Rupasinghe *et al.*, 2017). These components can affect the quality of the product, and volatile components can disturb the taste and smell of the final product, leading to possible applications of the final liquor in cocktails and general consumption (Pugliese *et al.*, 2013; Reboredo-Rodríguez *et al.*, 2015).

The amounts of citric acid, succinic acid, and acetic acid showed significant differences between the treatments with different concentrations of copoazú, while the concentrations of sugars glucose, ribose, and glycerol significantly differed between the treatments with different amounts of sugar. These results denote a stronger relationship between the amount of added sugar and complex sugars in copoazú and the amount of ethanol produced, including glycerol, as observed by other authors when fermenting fruit must (Vasantha Rupasinghe *et al.*, 2017). The amount of sucrose could have been due to incomplete fermentation because of the inhibitory factors mentioned above. However, this value was lower than that of glucose possibly because of the affinity of the strain used by the glucose, resulting in accelerated fermentation in the treatments with more added sugar. Similar results were found by Vasantha Rupasinghe *et al.* (2017) in fruit wines when studying the inhibition of by-products.

The chromatogram (Fig. 1) shows that the retention time of 16.8 min had a peak that corresponded to glycerol, leading to the question of whether everything that was fermented became ethanol or if glycerol was favored at some point in the metabolic pathway.

In kinetics, this serves as an inhibitory factor to produce ethanol and biomass (Fig. 2) as well as for substrate consumption (Vasantha Rupasinghe *et al.*, 2017), as reflected in the specific growth rate (Fig. 3).

Fermentation process

During the first stage of the fermentation process, the number of microorganisms and the amount of soluble solids remained stable. This phase is known as the adaptation phase of microorganisms, which is followed by a reduction in the number of soluble solids in the must (Fig. 2) and an increase in microorganisms. This is the exponential phase of the process, where both parameters stabilized in the final stage.

TABLE 4. Analysis of variance of the sugar and organic acids profile in the copoazú alcoholic beverages during the fermentation process.

Compound	Treatment (substrate concentration (g L^{-1}) / Soluble solids (ºBrix))					
	A (400 /15)	B (400/25)	C (400/35)	D (600/15)	E (600/25)	F (600/35)
Organic acids						
Citric	15.44 ± 0.43a	15.46 ± 0.82a	15.22 ± 1.23a	23.36 ± 0.9b	23.13 ± 0.31b	22.97 ± 0.03b
Pyruvic	0.55 ± 0.04a	0.57 ± 0.02a	0.54 ± 0.03a	0.83 ± 0.02a	0.81 ± 0.05a	0.81 ± 0.01a
Malic	1.85 ± 0.13a	1.84 ± 0.13a	1.88 ± 0.08a	2.87 ± 0.2a	2.69 ± 0.1a	2.72 ± 0.01a
Succinic	3.63 ± 0.23a	3.61 ± 0.24a	3.56 ± 0.08a	5.55 ± 0.31b	5.28 ± 0.33b	5.45 ± 0.06b
Lactic	0.54 ± 0.03a	0.56 ± 0.04a	0.53 ± 0.02a	0.83 ± 0.04a	0.84 ± 0.06a	0.84 ± 0.01a
Acetic	5.67 ± 0.30a	5.87 ± 0.05a	5.64 ± 0.25a	8.54 ± 0.29b	8.63 ± 0.33b	8.93 ± 0.01b
Sugars						
Sucrose	6.10 ± 0.28ab	4.22 ± 0.07a	0.65 ± 0.08c	3.25 ± 0.03b	1.45 ± 0.05d	0.72 ± 0.01c
Glucose	0.44 ± 0.04a	0.30 ± 0.01a	0.05 ± 0.01b	0.24 ± 0.01a	0.11 ± 0.00b	0.05 ± 0.01b
Ribose	2.94 ± 0.21a	2.10 ± 0.12a	0.31 ± 0.03b	1.59 ± 0.07c	0.71 ± 0.02b	0.35 ± 0.01b
Glycerol	14.13 ± 1.12a	9.70 ± 0.57b	1.54 ± 0.26c	7.44 ± 0.10c	3.32 ± 0.12d	1.66 ± 0.01c

n = 3. Measurements with the same letter do not show significant differences according to the ANOVA ($P<0.05$). All results are expressed in g of the substance fresh weight L^{-1}.

Quintero Mendoza, Díaz-Salcedo, and Hernández-Gómez: Design and development of a mixed alcoholic beverage kinetics using asaí (*Euterpe precatoria*) and copoazú (*Theobroma grandiflorum*)
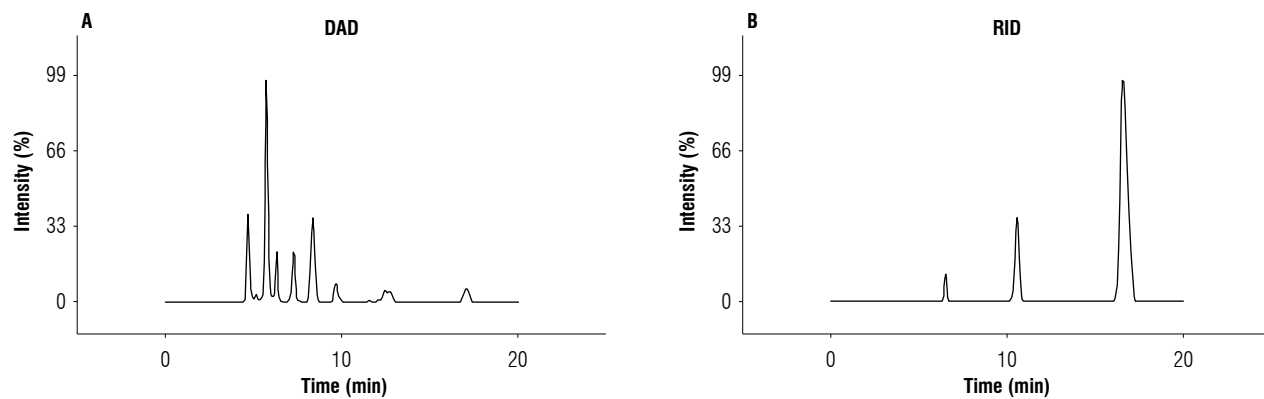
133

FIGURE 1. HPLC chromatogram for the profile of sugars and organic acids in the copoazú alcoholic beverages. A) DAD - Diode array detector; B) RID - refraction index detector.
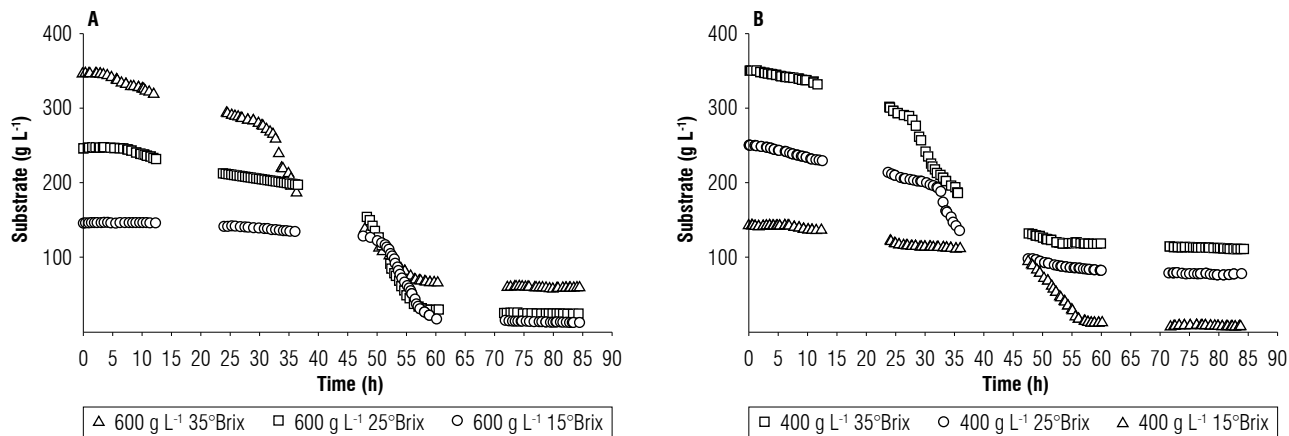

FIGURE 2. Comparison of fermentation performance with substrate variations at A) 600 g L^{-1} and B) 400 g L^{-1} of copoazú of different soluble solid content.
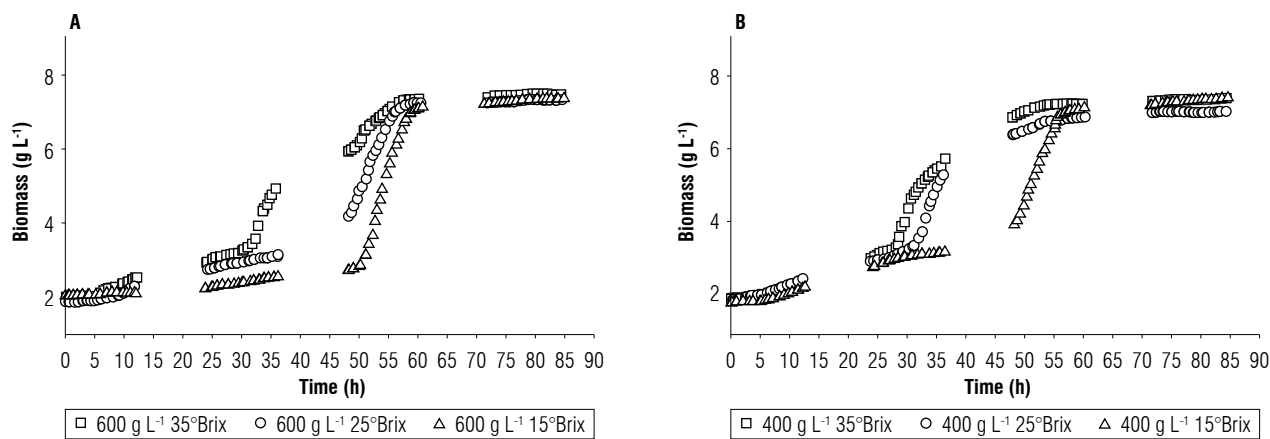

**FIGURE 3.** Comparison of fermentation performances for biomass variations at A) 600 g L^{-1} and B) 400 g L^{-1} of copoazú.

Figure 2 shows that the content of dissolved solids decreased considerably in the tests with less substrate because the microorganisms initially assimilated less complex sugars. Also, glucose is more easily assimilated by yeast than fructose, making it more effective at generating

alcohols from these sugars and inhibiting the production of glycerol. Similar results were found by Gao *et al.* (2018) and Zinnai *et al.* (2013) when working with *Saccharomyces cerevisiae* strains to produce wines. These authors observed that glycerol is generated under alkaline conditions, where

the metabolic pathway of glycerol-3-phosphatase is modified, causing phosphatase to react, forming glycerol. This means that the yeast needed a large amount of energy to convert glycerol into pyruvate and, in turn, pyruvate to ethanol (Arroyo-López, Querol, & Barrio, 2009; Vasantha Rupasinghe *et al.*, 2017).

For biomass (Fig. 3), growth followed the phases of microbial growth; in the exponential phase, growth was relatively fast when compared to the same types of fermentation because the biomass production was approximately 1% of the amount of substrate consumed, with an average of 2.89 ± 0.81%. This was possible because of the higher energy consumption caused by the increase in the amount of glycerol during fermentation (Arroyo-López, Orlić, *et al.*, 2009).

For the ethanol production (Fig. 4), the growth in relation to substrate consumption followed the following stoichiometry:

$$C_6H_{12}O_6 \rightarrow 2CH_3CH_2OH + 2CO_2$$
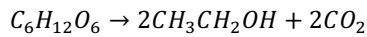
The ethanol yield, on average, varied between 47 and 65%, depending on the amount of substrate used. These results were relatively low because the yield of the conversion of sugars to ethanol was 95% on average (Zinnai *et al.*, 2013; Vasantha Rupasinghe *et al.*, 2017; Miller & Block, 2020), further indicating that glycerol may be inhibiting the metabolic process of fermentation. Nevertheless, fermentation reached contents higher than 20% ethanol; this allows subsequent mixing with dairy ingredients because the mixture did not need to be "fortified" with extra neutral alcohol to maintain the final alcohol content (Wardencki, 2019).

Fermentation kinetics parameters

Figures 5 and 6 show that the slope changed depending on the amount of added sugar (S_a), demonstrating the interdependence between these two variables. Therefore, linear

regressions with these slopes were proposed to consider the sugar content (Arroyo-López, Querol, & Barrio 2009; Miller & Block, 2020).
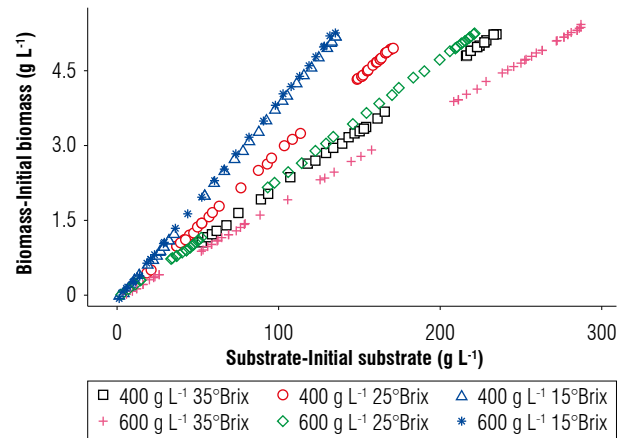

FIGURE 5. Evaluation of the experiment yields for the biomass/substrate interaction ($Y_{x/S}$) with a diagram of biomass formation versus substrate consumption.
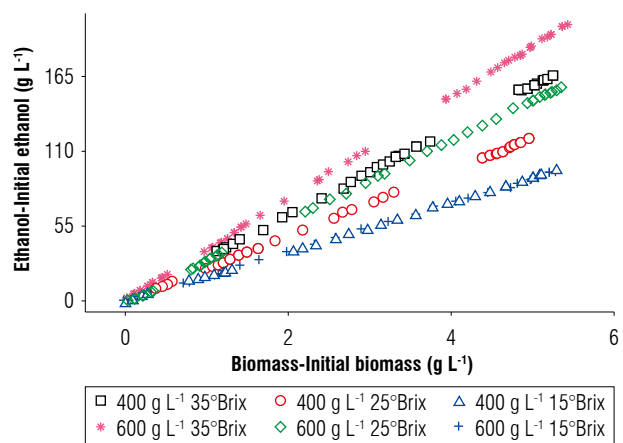

FIGURE 6. Evaluation of the experiment yields for the interaction of ethanol/biomass ($Y_{e/x}$) with a diagram of the formation of ethanol versus biomass.
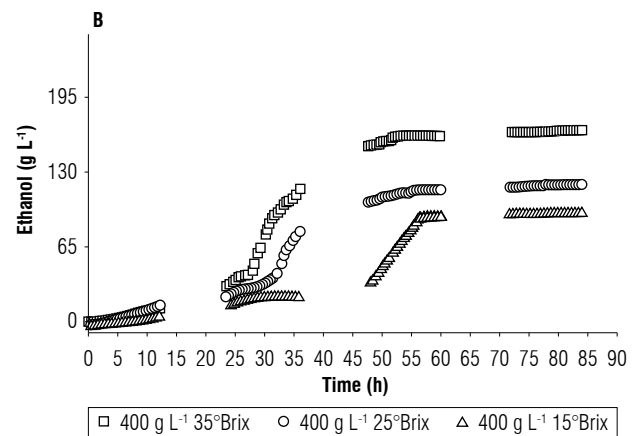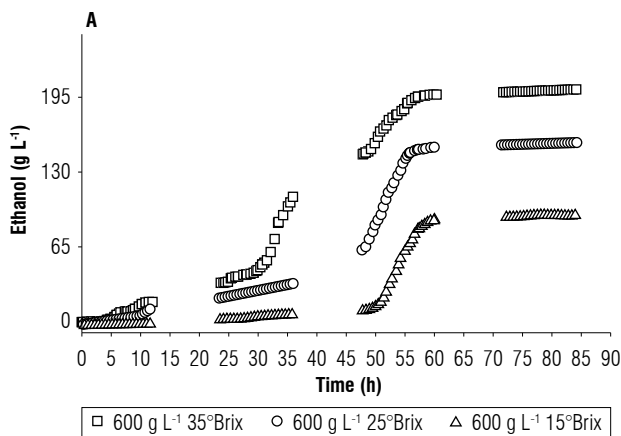

FIGURE 4. Comparison of fermentation yields for variations of ethanol at A) 600 g L^{-1} and B) 400 g L^{-1} of copoazú.

Quintero Mendoza, Díaz-Salcedo, and Hernández-Gómez: Design and development of a mixed alcoholic beverage kinetics using asaí (*Euterpe precatoria*) and copoazú (*Theobroma grandiflorum*)

135

Interaction between substrate and biomass:

$$Y_{\frac{x}{s}} = m_{\frac{x}{s}} S_a + b_{\frac{x}{s}} \qquad (7)$$

Interaction between ethanol and biomass:

$$Y_{\frac{e}{x}} = m_{\frac{e}{x}} S_a + b_{\frac{e}{x}} \qquad (8)$$

The data predicted the behavior of the biomass and substrate, calculating the missing factor, *i.e.*, the kinetic constant of the ethanol production (γ) through the reduction of least squares (Merger *et al.*, 2016).
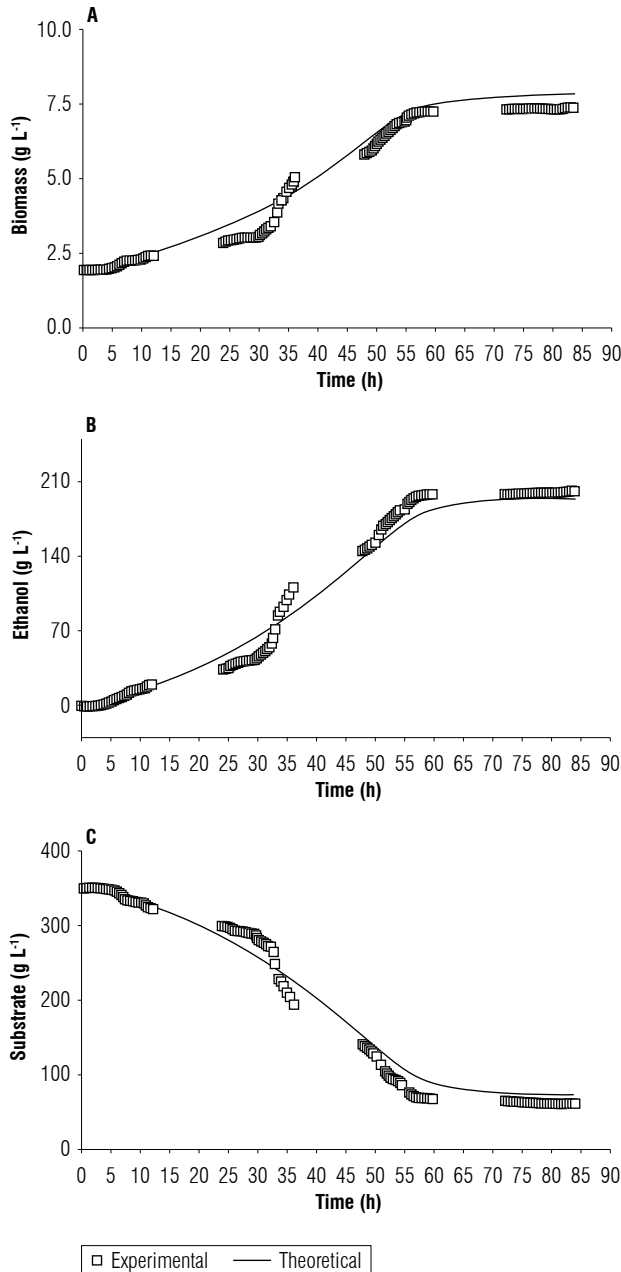

FIGURE 7. Evaluation of the variation between the kinetic model of fermentation and the experiment data for the contents of A) biomass, B) alcohol, and C) substrate in the fermentation of copoazú.

Fermentation kinetics parameters (Tab. 5) showed that the model adjusted favorably to the prediction of the experiment behavior of the substrate, biomass, and ethanol (Fig. 7). Additionally, the best yield was obtained with the treatment with 600 g L^{-1} of the substrate, adjusted with glucose at 35°Brix, and ending fermentation at approximately 60 h for subsequent maturation.

TABLE 5. Constants of the fermentation kinetics.

Constant			Value
Interaction between biomass and substrate	$Y_{x/S}$	$m_{x/S}$	-8.800E-05
		$b_{x/S}$	4.522E-02
Interaction between ethanol and biomass	$Y_{e/x}$	$m_{e/x}$	7.680E-02
		$b_{e/x}$	1.216E01
Ethanol production kinetic constant		γ	4.151E-03
Maximum specific growth rate		μ_{max}	6.061E-01
Saturation constant		K_s	1.328E03
Inhibition constant		K_i	3.861E-02
Adaptation constant		K_L	6.369E-05

Diffusion kinetics

Anthocyanin content and peroxide value of the asaí liqueur

The anthocyanin content initially increased and subsequently decreased (Fig. 8). For the asaí pulp, these readings resulted from the degradation of anthocyanins over time and the interaction processes with the pulp, reaching diffusive equilibrium. The lower anthocyanin content may have been due to the smaller transfer surface, although the drastic drop in a much shorter time compared to that of the pulp suggested that this behavior resulted from something in addition to the balance in the diffusion (Fig. 8) (Li *et al.*, 2017; Li *et al.*, 2018; Boeira *et al.*, 2020).
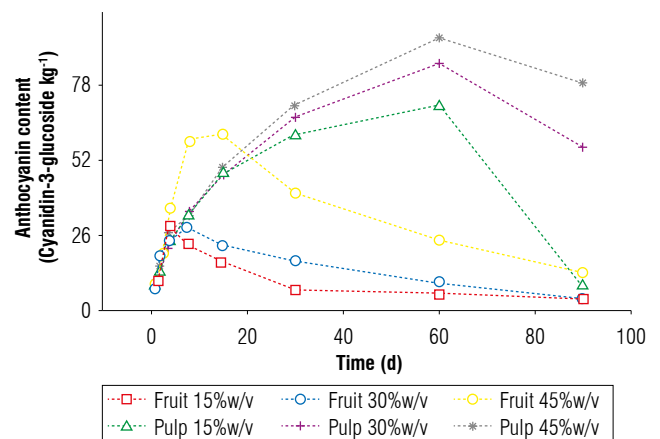

FIGURE 8. Anthocyanin content during the diffusive process of the asaí drink.

A lipid layer of fat was observed on the surface of the drinks because the fruits have a fat content of approximately 53% on a dry basis (Yuyama *et al.*, 2011; Castillo *et al.*, 2012). These lipids could contribute to oxidative rancidity, which was confirmed by measuring the acidity index of the fat in the beverages throughout the infusion, with changes in the index when the anthocyanin content decreased (Fig. 9). This demonstrated that the decrease in the antioxidant capacity and discoloration of the alcoholic beverages were strongly related to the rancidity of the fats in the liquor (Salaha *et al.*, 2008; Andersen & Skibsted, 2010; Peixoto *et al.*, 2016). This is why whole fruits were not utilized for the infusions and only the pulp was used, which had a lower percentage of fat that did not have a considerable negative effect on the drinks.
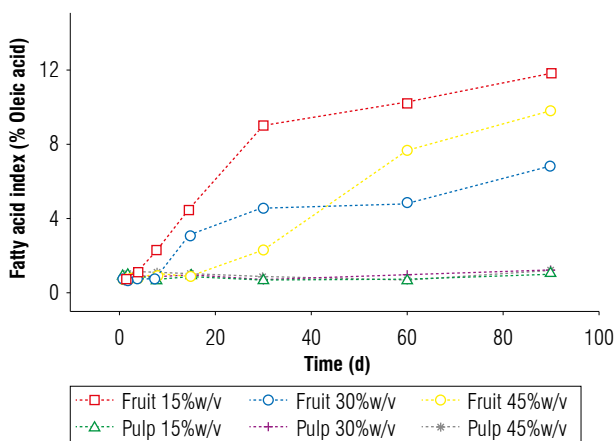

FIGURE 9. Fatty acid index during the diffusive process of the asaí drink.

Diffusion kinetics parameters

It was not possible to adjust the anthocyanin content data during diffusion (Fig. 8) to Fick's law, which is the most common model for diffusive processes since it has variables that affect the content of this metabolite. Therefore, a mathematical model was proposed to understand diffusion kinetics that considers the saturation or interaction of anthocyanins in the system and the deterioration of anthocyanins, either by lipids or light, using the following equation:

$$dC/dt = A + B + D + E \tag{9}$$

where A refers to the diffusive process originating from the pulp; this phenomenon is inversely proportional to time and depends on the initial pulp quantity, which is inversely proportional to the anthocyanin concentration in the beverage and to time. B refers to the interaction of anthocyanins within the drink, which is inversely proportional

to time; D is the degradation of these anthocyanins over time, which is inverse to the concentration of anthocyanins in the drink, and E is the transfer constant of this process (Shafirstein *et al.*, 2004; Chung *et al.*, 2016; 2017; Miller & Block, 2020). Each of these terms is expressed mathematically as follows, where C is the concentration expressed in mg of cyanidin-3-glucoside kg^{-1}, t is time in days, and dC/it is the variation of the concentration over time.

$$A = \frac{C_0 m_0 D_{PW}}{t} \tag{10}$$

where C_0 is the initial concentration of anthocyanins in the pulp, m_0 is the initial fresh mass of the pulp in kg, and D_{PW} is the diffusion constant.

$$B = \frac{K_I C}{t} \tag{11}$$

where K_I is the interaction or saturation constant.

$$D = -\frac{K_D t}{C} \tag{12}$$

where K_D is the decay constant.

$$E = K_t \tag{13}$$

where K_t is the transfer constant.

Replacing these terms in the equation provides:

$$\frac{dC}{dt} = \frac{C_0 m_0 D_{PW}}{t} + \frac{K_I C}{t} - \frac{K_D t}{C} + K_t \tag{14}$$

An evolutionary model was used to find the constants, which minimized the differences between the theoretical and experimental data. The initial values used for the estimation were obtained from the mean values of the segmented slopes of the experiment data, using the interaction constant for the diffusion constant from d 1 to 4, the transfer constant from d 4 to 15, the interaction constant from d 15 to 60, and the decay constant from d 60 to 90, obtaining the values in Table 6.

TABLE 6. Diffusion kinetics constants of the asaí infusion process.

Constant		Value
Diffusion constant	D_{PW}	1.090E-06
Interaction constant	K_i	5.091E-01
Decay constant	K_D	2.190
Transfer constant	K_t	8.418E-01

These parameters, when applied and compared to the experiment data, showed no significant difference (Fig. 10).
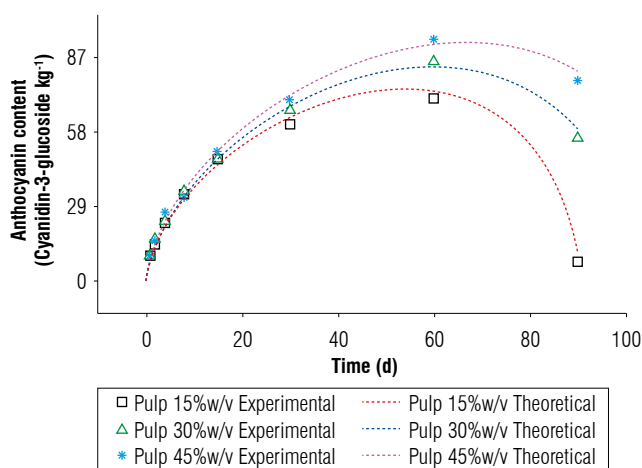
FIGURE 10. Evaluation of the variation between the diffusive model and the experiment data for the diffusion of asaí in the alcoholic beverage.

Conclusions

This study developed kinetic models for copoazú fermentation and asaí diffusion process, to obtain optimum liquor in each case.

In the copoazú liquor, ethanol production was favored by more complex sugars since they delay the inhibition process, either with ethanol or glycerol. The dependence of both products was evidenced in the values of the inhibition and saturation constants that defined the specific growth rate that, in turn, considerably affected the rate of change for the biomass, substrate, and alcohol. The best yield was observed with 600 g L^{-1} of copoazú pulp and glucose at 35 °Brix, achieving yields of up to 20% w/v in the alcohol content.

In the asaí liquor, when the fruit was used instead of the pulp, the fruit lipids caused unfavorable reactions that deteriorated the organoleptic and sensory properties of the liquor. This is an important factor in the relationship between the interaction constant and the decay constant since they define the turning point in the predictive behavior of the anthocyanin content, with the maximum near d 60. The best behavior was seen with the pulp at 45% (w/v) since the greater surface facilitated the exchange and transfer of mass. Additionally, a lower fat content was recorded, thus avoiding rancidity that deteriorates organoleptic characteristics. Anthocyanin content proves to be a good marker of beverage properties deterioration.

Acknowledgments

Conflict of interest statement

The authors declare that there is no conflict of interest regarding the publication of this article.

Author's contributions

WQM formulated the overarching research goals and aims, conducted the research process, performed the experiments, managed and coordinated the research activity planning and execution, analyzed the study data, designed the methodology, and created the models. RODS designed the methodology and carried out the manuscript's critical review. MSHG obtained the financial support for the project leading to this publication, designed the methodology, and carried out the manuscript's critical review.

Literature cited

Andersen, M. L., & Skibsted, L. H. (2010). Light-induced quality changes in food and beverages. In L. H. Skibsted, J. Risbo, & M. L. Andersen (Eds.), *Chemical deterioration and physical instability of food and beverages* (pp. 113–139). Woodhead Publishing. https://doi.org/10.1533/9781845699260.1.113

Arroyo-López, F. N., Orlić, S., Querol, A., & Barrio, E. (2009). Effects of temperature, pH, and sugar concentration on the growth parameters of *Saccharomyces cerevisiae*, *S. kudriavzevii*, and their interspecific hybrid. *International Journal of Food Microbiology*, *131*(2–3), 120–127. https://doi.org/10.1016/j.ijfoodmicro.2009.01.035

Arroyo-López, F. N., Querol, A., & Barrio, E. (2009). Application of a substrate inhibition model to estimate the effect of fructose concentration on the growth of diverse *Saccharomyces cerevisiae* strains. *Journal of Industrial Microbiology and Biotechnology*, *36*(5), 663–669. https://doi.org/10.1007/s10295-009-0535-x

Bermejo, C., Haerizadeh, F., Takanaga, H., Chermak, D., & Frommer, W. B. (2011). Optical sensors for measuring dynamic changes of cytosolic metabolite levels in yeast. *Nature Protocols*, *6*, 1806–1817. https://doi.org/10.1038/nprot.2011.391

Boeira, L. S., Bastos Freitas, P. H., Uchôa, N. R., Bezerra, J. A., Cád, S. V., Duvoisin Junior, S., Albuquerque, P. M., Mar, J. M., Ramos, A. S., Machado, M. B., & Maciel, L. R. (2020). Chemical and sensorial characterization of a novel alcoholic beverage produced with native acai (*Euterpe precatoria*) from different regions of the Amazonas state. *LWT*, *117*, Article 108632. https://doi.org/10.1016/j.lwt.2019.108632

Carrillo Bautista, M. P., Cardona Jaramillo, J. E. C., Barrera García, J. A., & Hernández Gómez, M. S. (2016). *Colombia: frutas de la Amazonia*. Instituto Amazónico de Investigaciones Científicas - SINCHI, Ministerio de Ambiente y Desarrollo Sostenible.

Carrillo Bautista, M. P., Cardona Jaramillo, J. E. C., Diaz Salcedo, R. O., Orduz Díaz, L. L., Peña Rojas, L. F., Hernández Gómez, M. S., & Mosquera Narváez, L. E. (2017). *Los ingredientes naturales de la Amazonia colombiana: sus aplicaciones y especificaciones*

técnicas (1st ed.). Instituto Amazónico de Investigaciones Científicas - SINCHI, Ministerio de Ambiente y Desarrollo Sostenible.

Castillo Quiroga, Y. M., Hernández Gómez, M. S., & Lares, M. (2017). Componentes bioactivos del asai (*Euterpe oleracea* Mart. y *Euterpe precatoria* Mart.) y su efecto sobre la salud. *Archivos Venezolanos de Farmacología y Terapéutica*, *36*(3), 58–66.

Castillo, Y. M., Lares, M., & Hernández, M. S. (2012). Caracterización bromatológica y fisicoquímica del fruto amazónico asaí (*Euterpe precatoria* Mart.). *Vitae*, *19*(1), S309–S311.

Chung, C., Rojanasasithara, T., Mutilangi, W., & McClements, D. J. (2016). Stabilization of natural colors and nutraceuticals: inhibition of anthocyanin degradation in model beverages using polyphenols. *Food Chemistry*, *212*, 596–603. https://doi.org/10.1016/j.foodchem.2016.06.025

Chung, C., Rojanasasithara, T., Mutilangi, W., & McClements, D. J. (2017). Stability improvement of natural food colors: impact of amino acid and peptide addition on anthocyanin stability in model beverages. *Food Chemistry*, *218*, 277–284. https://doi.org/10.1016/j.foodchem.2016.09.087

Comelli, R. N., Seluy, L. G., & Isla, M. A. (2016). Performance of several *Saccharomyces* strains for the alcoholic fermentation of sugar-sweetened high-strength wastewaters: comparative analysis and kinetic modelling. *New Biotechnology*, *33*(6), 874–882. https://doi.org/10.1016/j.nbt.2016.09.007

Cuellar Álvarez, L., Cuellar Álvarez, N., Galeano García, P., & Suárez Salazar, J. C. (2017). Effect of fermentation time on phenolic content and antioxidant potential in Cupuassu (*Theobroma grandiflorum* (Willd. ex Spreng.) K. Schum.) beans. *Acta Agronómica*, *66*(4), 473–479. https://doi.org/10.15446/acag.v66n4.61821

Dias, D. R., Duarte, W. F., & Schwan, R. F. (2017). Methods of evaluation of fruit wines. In M. R. Kosseva, V. K. Joshi, & P. S. Panesar (Eds.), *Science and technology of fruit wine production* (pp. 227–252). Academic Press. https://doi.org/10.1016/B978-0-12-800850-8.00005-3

Duarte, W. F., Dias, D. R., Oliveira, J. M., Teixeira, J. A., Almeida e Silva, J. B., & Schwan, R. F. (2010). Characterization of different fruit wines made from cacao, cupuassu, gabiroba, jaboticaba and umbu. *LWT - Food Science and Technology*, *43*(10), 1564–1572. https://doi.org/10.1016/j.lwt.2010.03.010

Gao, Y. T., Zhang, Y. S., Wen, X., Song, X. W., Meng, D., Li, B. J., Wang, M. Y., Tao, Y. Q., Zhao, H., Guan, W. Q., & Du, G. (2018). The glycerol and ethanol production kinetics in low-temperature wine fermentation using *Saccharomyces cerevisiae* yeast strains. *International Journal of Food Science and Technology*, *54*(1), 102–110. https://doi.org/10.1111/ijfs.13910

Kumar, S., Dheeran, P., Singh, S. P., Mishra, I. M., & Adhikari, D. K. (2013). Kinetic studies of ethanol fermentation using *Kluyveromyces* sp. IIPE453. *Journal of Chemical Technology and Biotechnology*, *88*(10), 1874–1884. https://doi.org/10.1002/jctb.4042

Li, H., Wang, H., Li, H., Goodman, S., van der Lee, P., Xu, Z., Fortunato, A., & Yang, P. (2018). The worlds of wine: old, new and ancient. *Wine Economics and Policy*, *7*(2), 178–182. https://doi.org/10.1016/j.wep.2018.10.002

Li, S., An, Y., Fu, W., Sun, X., Li, W., & Li, T. (2017). Changes in anthocyanins and volatile components of purple sweet potato fermented alcoholic beverage during aging. *Food Research International*, *100*(2), 235–240. https://doi.org/10.1016/j.foodres.2017.08.041

Merger, J., Borzì, A., & Herzog, R. (2016). Optimal control of a system of reaction-diffusion equations modeling the wine fermentation process. *Optimal Control Applications and Methods*, *38*(1), 112–132. https://doi.org/10.1002/oca.2246

Miller, G. H. (2019). *Whisky science. A condensed distillation.* Springer. https://doi.org/10.1007/978-3-030-13732-8

Miller, K. V., & Block, D. E. (2020). A review of wine fermentation process modeling. *Journal of Food Engineering*, *273*, Article 109783. https://doi.org/10.1016/j.jfoodeng.2019.109783

Miranda Castilleja, D. E., Aldrete Tapia, J. A., Arvizu Medrano, S. M., Hernández Iturriaga, M., Soto Muñoz, L., & Martínez Peniche, R. Á. (2017). Growth kinetics for the selection of yeast strains for fermented beverages. In A. Morata, & I. Loira (Eds.), *Yeast - industrial applications*. IntechOpen. https://doi.org/10.5772/intechopen.70224

Peixoto, H., Roxo, M., Krstin, S., Röhrig, T., Richling, E., & Wink, M. (2016). An anthocyanin-rich extract of Acai (*Euterpe precatoria* Mart.) increases stress resistance and retards aging-related markers in *Caenorhabditis elegans*. *Journal of Agricultural and Food Chemistry*, *64*(6), 1283–1290. https://doi.org/10.1021/acs.jafc.5b05812

Pugliese, A. G., Tomas-Barberán, F. A., Truchado, P., & Genovese, M. I. (2013). Flavonoids, proanthocyanidins, vitamin C, and antioxidant activity of *Theobroma grandiflorum* (cupuassu) pulp and seeds. *Journal of Agricultural and Food Chemistry*, *61*(11), 2720–2728. https://doi.org/10.1021/jf304349u

Reboredo-Rodríguez, P., González-Barreiro, C., Rial-Otero, R., Cancho-Grande, B., & Simal-Gándara, J. (2015). Effects of sugar concentration processes in grapes and wine aging on aroma compounds of sweet wines - a review. *Critical Reviews in Food Science and Nutrition*, *55*(8), 1053–1073. https://doi.org/10.1080/10408398.2012.680524

Salaha, M. I., Kallithraka, S., Marmaras, I., Koussissi, E., & Tzourou, I. (2008). A natural alternative to sulphur dioxide for red wine production: influence on colour, antioxidant activity and anthocyanin content. *Journal of Food Composition and Analysis*, *21*(8), 660–666. https://doi.org/10.1016/j.jfca.2008.03.010

Shafirstein, G., Bäumler, W., Lapidoth, M., Ferguson, S., North, P. E., & Waner, M. (2004). A new mathematical approach to the diffusion approximation theory for selective photothermolysis modeling and its implication in laser treatment of port-wine stains. *Lasers in Surgery and Medicine*, *34*(4), 335–347. https://doi.org/10.1002/lsm.20028

Topalovic, A., & Mikulic-Petkovsek, M. (2010). Changes in sugars, organic acids and phenolics of grape berries of cultivar Cardinal during ripening. *Journal of Food, Agriculture and Environment*, *8*(3–4), 223–227.

United States Pharmacopeial Convention. (2013). *USP36 NF31, 2013: U.S. pharmacopeia national formulary* (Vol. 1). U.S. Pharmacopeia.

Vasantha Rupasinghe, H. P., Joshi, V. K., Smith, A., & Parmar, I. (2017). Chemistry of fruit wines. In M. R. Kosseva, V. K.

Joshi, & P. S. Panesar (Eds.), *Science and technology of fruit wine production* (pp. 105–176). Academic Press. https://doi.org/10.1016/B978-0-12-800850-8.00003-X

Wardencki, W. (2019). Alcoholic beverages. In P. Worsfold, C. Poole, A. Townshend, & M. Miró (Eds.), *Encyclopedia of Analytical Science* (3rd. ed., pp. 67–76). Elsevier. https://doi.org/10.1016/B978-0-12-409547-2.14330-6

Yuyama, L. K. O., Aguiar, J. P. L., Silva Filho, D. F., Yuyama, K., Varejão, M. J., Fávaro, D. I. T., Vasconcellos, M. B. A., Pimentel, S.

A., & Caruso, M. S. F. (2011). Caracterização físico-química do suco de açaí de *Euterpe precatoria* Mart. oriundo de diferentes ecossistemas amazônicos. *Acta Amazonica*, *41*(4), 545–552. https://doi.org/10.1590/S0044-59672011000400011

Zinnai, A., Venturi, F., Sanmartin, C., Quartacci, M. F., & Andrich, G. (2013). Kinetics of D-glucose and D-fructose conversion during the alcoholic fermentation promoted by *Saccharomyces cerevisiae*. *Journal of Bioscience and Bioengineering*, *115*(1), 43–49. https://doi.org/10.1016/j.jbiosc.2012.08.008